

## Local Pool Boiling Coefficients on Horizontal Tubes

Myeong-Gie Kang\*

Department of Mechanical Engineering Education, Andong National University,  
388 Songchun-dong, Andong-city, Kyungbuk 760-749, Korea

Local pool boiling on the outside and inside surfaces of a 51 mm diameter tube in horizontal direction has been studied experimentally in saturated water at atmospheric pressure. Much variation in local heat transfer coefficients was observed along the tube periphery. On the outside surface the maximum and the minimum are observed at  $\theta=45^\circ$  and  $180^\circ$ , respectively. However, on the inside surface only the minimum was observed at  $\theta=0^\circ$ . Major mechanisms on the outside surface are liquid agitation and bubble coalescence while those on the inside surface are micro layer evaporation and liquid agitation. As the heat flux increases liquid agitation gets effective both on outside and inside surfaces. The local coefficients measured at  $\theta=90^\circ$  can be recommended as the representative values of both outside and inside surfaces.

**Key Words :** Pool Boiling, Annuli, Horizontal Tube, Heat Transfer

### Nomenclature

$A$	Heat transfer area
$D$	Tube diameter
$h_b$	Boiling heat transfer coefficient
$I$	Supplied current
$L$	Heated tube length
$q$	Input power
$q''$	Heat flux
$T_{sat}$	Saturated water temperature
$T_w$	Tube surface temperature
$V$	Supplied voltage
$\Delta T_{sat}$	Degree of superheating ( $= T_w - T_{sat}$ )
$\theta$	Azimuthal angle along the tube periphery

### 1. Introduction

Mechanisms of pool boiling heat transfer have been investigated in nuclear power plants for the purpose of acquiring inherent safety functions (Kang, 2001). To design more efficient heat exchangers, effects of several parameters on heat

transfer must be studied in detail. The horizontal direction can be regarded as a possible choice. Since much difference exists in surface temperatures along the tube circumference (Jung et al., 1987, Kang, 2000), suggesting a boiling heat transfer coefficient of a tube without denoting its location could be a cause of discrepancy in previous results of horizontal tubes.

Some previous studies on local heat transfer coefficients on the circular shape in horizontal location are summarized in Table 1. Types of the heating geometry are tubes, hemispheres, and a flat plate. Cornwell and Einarsson (1990) and Gupta et al (1995) studied both pool and flow boiling. Studies on local coefficients by Lance and Myers (1958) report that the type of boiling liquid can change the trend of local coefficients along the tube periphery. As the liquid is methanol the maximum local coefficient was observed at the tube bottom while the maximum was at the tube sides as the boiling liquid was n-hexane. Cornwell and Einarsson (1990) reported that the maximum local coefficient was observed at the tube bottom, as the boiling liquid was R-113. The location of the maximum heat transfer coefficient moves toward tube sides as the fluid flow around the tube increases. Cornwell and Houston (1994)

\* E-mail mgkang@andong.ac.kr

TEL +82-54-820-5483, FAX +82-54-823-1766

Department of Mechanical Engineering Education,  
Andong National University, 388 Songchun-dong,  
Andong-city, Kyungbuk 760-749, Korea (Manuscript

Received August 29, 2004, Revised January 20, 2005)

Table 1 Items and categories of the river landscape

Category	Author	Geometry	Material	Fluid	Boiling condition
Outside surface	Lance and Myers (1958)	1.25 in tube 2 in tube	Copper	Methanol n-hexane	Pool boiling
	Cornwell and Ernäs (1990)	27.1 mm tube	Thin stainless steel sleeve on a copper rod	R-113	Flow boiling Pool boiling
	Cupta et al (1995)	19.05 mm tube bundle	Stainless steel	Water	Flow boiling Pool boiling
	El-Genk and Gao (1999)	15.2 mm dia hemisphere	Aluminum Stainless steel	Water	Pool boiling
	Cheung et al (1999)	0.305 m dia hemisphere	Aluminum	Water	Pool boiling
	Kong (2000)	19.05 mm tube	Stainless steel	Water	Pool boiling
Inside surface	Jung et al (1987)	Circular flat plate of 7.8 cm diameter	Copper	R-11	Pool boiling
	Jabardo and Filho (2000)	12.7 mm tube	Copper	R-22 R-134a R-404A	Pool boiling

explained the reason of the difference in local coefficients along the circumference by sliding bubbles.

According to Gupta et al (1995), as the liquid is water, the maximum and the minimum local coefficients are observed at the bottom and top regions of the tube circumference, respectively. Kang (2000) reported the similar results using the same tube diameter and liquid. Gupta et al (1995) studied azimuthal angles ( $\theta$ ) of every 45° along the tube periphery while Kang (2000) studied only three angles of 0°, 90°, and 180°. However, comparing two results quantitatively is not reasonable since the test sections in Gupta et al (1995) and Kang (2000) were a tube bundle and a single tube, respectively. Therefore, it is still necessary to study more azimuthal angles on a single tube circumference.

Results by El-Genk and Gao (1999) and Cheung et al (1999) also reported that local coefficients on a hemisphere were changing along the circumference of a hemisphere. Much difference was observed between two local values at the bottom and sides.

Although some researchers have published results of pool boiling on the outside surface, the study for the inside surface of a tube is very rare. Jung et al (1987) experimented boiling of R-11 to investigate heat transfer mechanisms on the inside surface of a circular cylindrical tank. They simulated the surface with a flat plate. That is, the plate facing downward simulated the uppermost region of the surface. Somewhat detailed study on the inclination angle itself was previously done by Nishikawa et al (1984). To simulate a circular tank by a flat plate might be reasonable in a sense as the diameter of the tank was large enough. However, it is doubtful to use the results for the design of tubular heat exchangers. Jabardo and Filho (2000) performed an experimental study of forced convective boiling of refrigerants in a 12.7 mm internal diameter copper tube. They investigate effects of physical parameters over the variations in local surface temperature as a function of the fluid quality. However, mechanisms of pool boiling are different from those of the forced convective boiling.

In addition to the analyses on local boiling

coefficients one of the most important subjects is to propose a method of defining the representative coefficient. Among the previous results only Kang (2000) suggested a way of determining the representative temperature. According to Kang (2000) the temperatures measured on the side ( $\theta=90^\circ$ ) of a horizontal tube can be treated as a representative value on the outside surface of a horizontal tube.

Through the analysis of the published results, the present study is aimed at (1) to improve Kang's previous results, (2) to investigate local coefficients on the inside surface for the first time, and (3) to recommend the representative local coefficient on a horizontal tube.

## 2. Experiments

A schematic view of the present experimental apparatus is shown in Fig. 1. The water storage tank is made of stainless steel and has a rectangular cross section ( $950 \times 1300$  mm) and a height of 1400 mm. This tank has a glass view port ( $1000 \times 1000$  mm) which permits viewing of the tubes and photographing. The inside tank has several flow holes to allow fluid inflow from the outer tank. To reduce heat loss to the environment, the left, right, and rear sides of the tank were insulated by glass wool of 50 mm thickness.

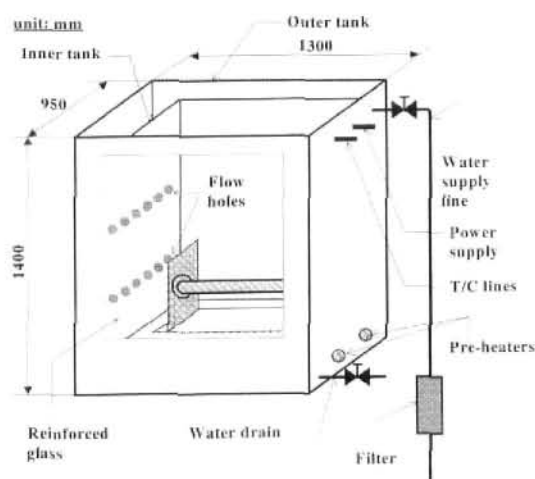


Fig. 1 Schematic of the experimental apparatus

Figure 2 shows a test section and a supporter for the outside surface heating tests. Resistance heaters simulated the heat exchanger tubes. Several rows of resistance wires are arrayed uniformly inside the heated tube to supply power to the tube. The surface of the tube was finished through buffing process to have smooth surface. Figure 3 shows a test section and a supporter for the inside surface heating tests. Several rows of resistance wires are arrayed uniformly around the outside surface of the heated tube. Then, the wires were covered with insulating material. The inside surface was lathed to have smooth surface. Both heated tubes are made of stainless steel and the heated length ( $L$ ) and the diameter ( $D$ ) are 300 and 51 mm, respectively.

Temperatures of the outside surface heating tests were instrumented with five T-type sheathed thermocouples (diameter is 1.5 mm). The thermocouple tip (about 10 mm) was bent at a 90-degree angle and the bent tip brazed on the tube wall as shown in Fig. 2(a). For the inside sur-

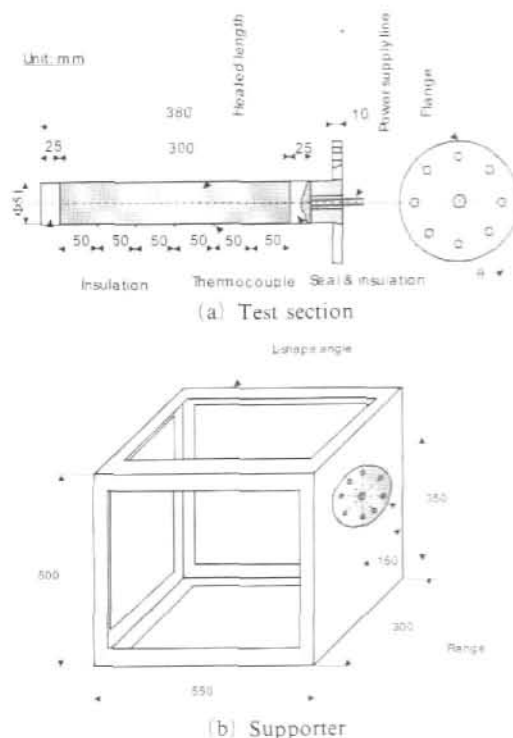


Fig. 2 Text section and its supporter for outside surface tests

face heating tests, temperatures on the outside surface of the heated tube were measured with two T-type sheathed thermocouples (diameter is 1 mm) located at 100 mm distance from both ends of the heated tube. The temperatures of the inside tube surface were calculated by the one dimensional conduction equation. To install the thermocouples on the surface two grooves (width $\times$ depth=1 mm $\times$ 1 mm) of 105 mm length were manufactured on the surface. The water temperatures were measured with six sheathed T-type thermocouples placed at the tank wall vertically from the bottom of the inside tank with equal spacing (i.e., 180 mm).

For the tests, the assembled part is placed at the bottom of the tank (Fig. 1). After the tank is filled with water until the initial water level is at 750 mm from the outer tank bottom, the water is heated using four pre-heaters at constant power (5 kW/heater). When the water temperature reaches the saturation value (100°C since all the tests are run at atmospheric pressure), the water is then boiled for 30 minutes at saturation temperature to remove the dissolved gases. The temperatures of the heated tube are measured when they are at steady state while controlling the heat flux on the tube surface with input power. To make

the azimuthal angle, one or both sides of the test section have flanges. The peripheral variation in heat transfer was determined by rotating the tube following each set of readings.

The error bound of the voltage and current meters used for the test are  $\pm 0.5\%$  of the measured value. Therefore, the calculated power (voltage $\times$ current) has  $\pm 1.0\%$  error bound. Since the heat flux ( $q''$ ) has the same error bound as the power, the uncertainty in the heat flux is estimated to be  $\pm 1.0\%$ . The measured temperature has uncertainties originated from the thermocouple probe itself and the instrument. To evaluate the error bound of the thermocouple probe, three thermocouples brazed on tube surface were submerged in an isothermal bath of  $\pm 0.01$  K accuracy. The measured temperatures were compared with the set temperature. The deviation between the values is within  $\pm 0.1$  K inclusive of the bath accuracy. The error bound of the data acquisition system is  $\pm 0.05$  K. Therefore, the total uncertainty of the measured temperatures is defined by adding the above errors and its value is  $\pm 0.15$  K.

The largest heat transfer occurred at  $q''=50$  kW/m<sup>2</sup> for the outside surface heating tests. For the case, the maximum temperature difference is 1.8 K between the temperatures at  $\theta=45^\circ$  and  $180^\circ$ . The one dimensional conduction heat transfer along the tube periphery is calculated as 0.45 kW/m<sup>2</sup>. This value is just 0.9% of the radial heat flux. Moreover, as the heat flux is more or less than 50 kW/m<sup>2</sup>, the amount of the peripheral heat flux is decreasing. Since the amount of peripheral heat transfer along the outside surface is not very large, its effect on the local heat transfer coefficients has been neglected.

The heat flux along the inside tube periphery has been evaluated by using one-dimensional conduction equation. The maximum possible heat flux is 2.3 kW/m<sup>2</sup> as the tube wall superheat ( $\Delta T_{sat}$ ) is 4 K. The value is about 11% of the averaged radial heat flux (40 kW/m<sup>2</sup>). This can result in additional  $\pm 10\%$  uncertainty in the heat flux. The axial heat loss from the ends of the test section is also calculated and is less than 30 W (e.g., 24 W at  $q''=91$  kW/m<sup>2</sup> and  $\theta=0^\circ$ ).

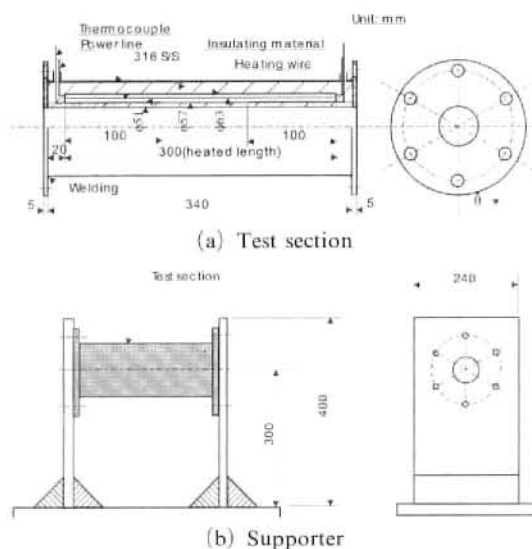


Fig. 3 Test section and its supporter for inside surface tests

Since this is very small comparing with the radial heat transfer (e.g., 4.4 kW at  $q''=91 \text{ kW/m}^2$ ), its effect on the heat transfer coefficient is neglected.

The heat flux from the electrically heated tube surface is calculated from the measured values of the AC power input as follows :

$$q'' = \frac{VI}{\pi DL} = h_b(T_w - T_{sat}) = h_b \Delta T_{sat} \quad (1)$$

where  $V$  and  $I$  are the supplied voltage (in volt) and current (in ampere), and  $D$  and  $L$  are the tube diameter and the length of the heated tube, respectively.  $T_w$  and  $T_{sat}$  represent the temperatures of the tube surface and the saturated water, respectively.

### 3. Results and Discussion

Figure 4(a) shows variations in local heat transfer coefficients on the outside surface of the tube as the heat flux is changing.  $h_b$  increases as  $\theta$  is changing from  $0^\circ$  to  $45^\circ$ . Then, it is decreasing continuously until  $\theta$  gets  $180^\circ$ . The maximum and the minimum local coefficients are observed at  $\theta=45^\circ$  and  $180^\circ$ , respectively. The maximum point is somewhat different from Gupta et al. (1995). However, precise observation on the Gupta et al.'s experimental data of no cross flow says that the maximum point is highly dependent on the tube location and the heat flux. Some data sets are showing its maximum at  $\theta=45^\circ$ . Therefore, it can be said that geometrical difference can be regarded as a major cause of the difference since the difference could result in flow difference around the tube. At  $q''=60 \text{ kW/m}^2$  the local coefficient increases more than 35% as  $\theta$  changes from  $180^\circ$  to  $45^\circ$ . The major cause of the increase of the local coefficient is the liquid agitation due to sliding bubbles (Kang, 2000; Cornwell and Houston, 1994). Effects of liquid agitation on heat transfer get decreasing as the azimuthal angle increases more than  $90^\circ$ . The bubbles from lower regions move toward the upper regions along the tube periphery and generate bigger bunches of bubbles around the uppermost regions. The coalesced bubbles prevent access of relevant liquid to the heated surface and result in heat transfer

decrease at the regions. Moreover, since bubbles coming from the lower regions are moving to upward due to buoyancy, bubbles begin to departure from the tube as  $\theta \geq 90^\circ$ . This accelerates the generation of bubble coalescence and decreases the intensity of liquid agitation. At lowermost region of the tube, heat transfer is dependent on the nucleation sites density and the circulating flow in the tank. The maximum and minimum heat transfer coefficients are measured at the places where the maximum liquid agitation

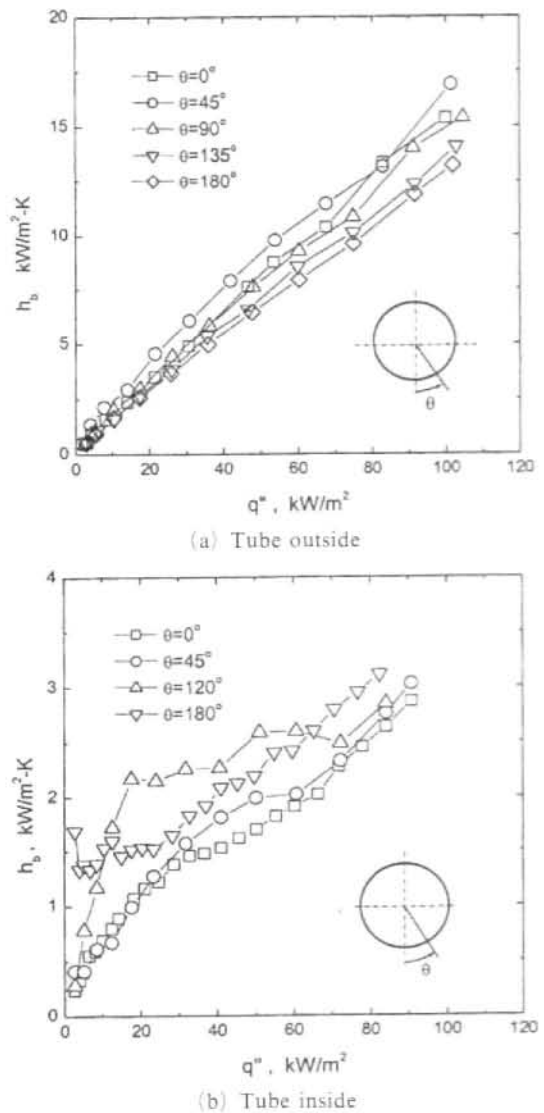


Fig. 4 Local heat transfer coefficients due to the heat flux change

( $\theta=45^\circ$ ) and the maximum bubble coalescence ( $\theta=180^\circ$ ) are expected, respectively. The location of the maximum heat transfer is expected to move to the lower azimuthal angles as the heat flux increases. Some photos of saturated boiling on the outside surface of the tube are shown in Fig. 5. The density of bubbles is increasing gradually and the formation of bubble slugs is observed as the heat flux increases. Observing the photos of the tube circumference the region of bubble slug is increasing toward tube sides as the heat flux increases.

Figure 4(b) shows variations in local coefficients on the inside surface. At  $\theta=0^\circ$  and  $45^\circ$  the intensity of liquid agitation is very weak at lower heat fluxes. Regions at  $\theta=0^\circ$  and  $45^\circ$  are relatively free from the liquid agitation at low and medium heat fluxes since bubbles are just moving upward. Therefore, the major mechanism affecting on heat transfer is the density of nucleation

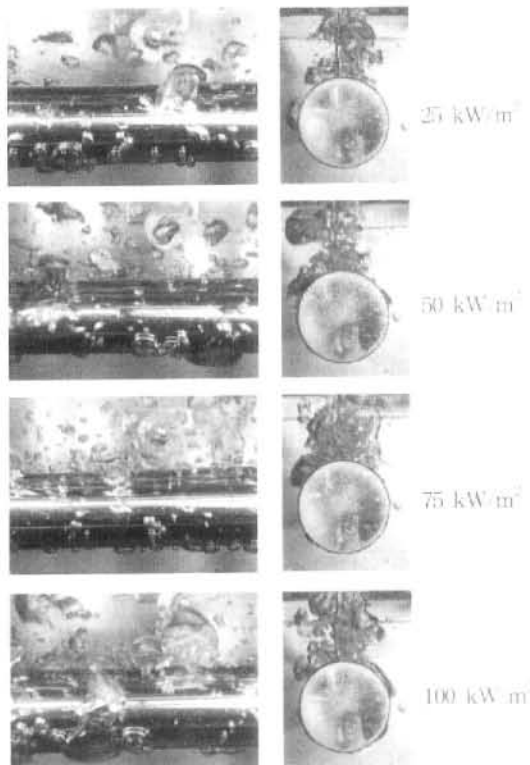
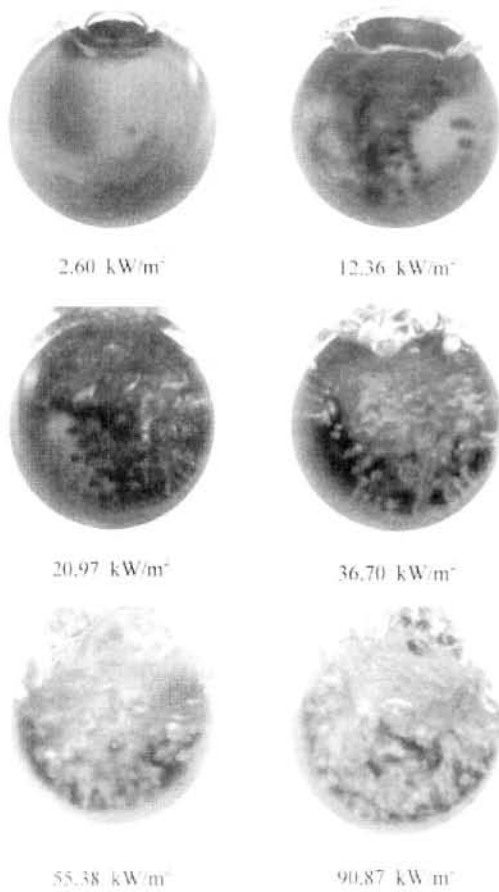


Fig. 5 Photos of saturated pool boiling on the outside surface

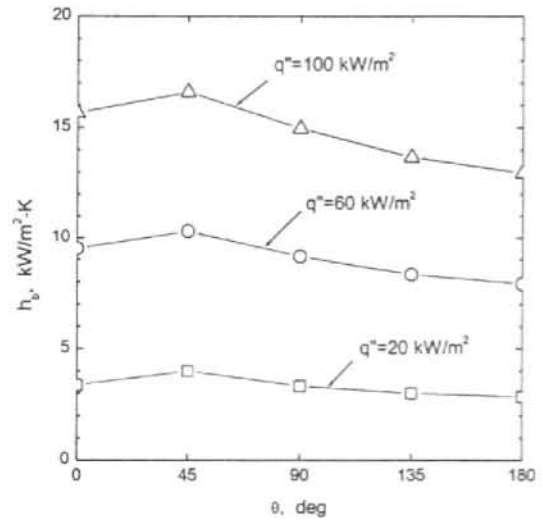
sites. At  $\theta=120^\circ$  the intensity of the liquid agitation is strongly affecting on heat transfer at lower heat fluxes less than  $18 \text{ kW/m}^2$ . The source of the liquid agitation is bubbles coming from the bottom of the tube. As the heat flux increases more than  $18 \text{ kW/m}^2$  this region is nearby the boundary of an elongated bubble. The intensity of the liquid agitation decreases suddenly and bubbles become coalescing around this angle. At  $\theta=180^\circ$ , the higher coefficient was observed at a very low heat flux nearby 0. This is very unusual regarding the previously published results for the several geometries. The departed bubbles from the tube bottom and side regions move upward and coalesce at the uppermost regions of the tube inside to generate a very large elongated bubble underneath the surface. The existence of a micro liquid layer between the tube surface and the elongated bubble and its evaporation is the major cause of the higher heat transfer coefficient. As the bubble flows out from the ends of the tube, environmental liquid rushes into the space and, accordingly, the active liquid agitation is generated inside the tube. Therefore, the higher heat transfer coefficient at low heat fluxes can be explained by both of the evaporative mechanism (Hewitt, 1978) underneath the elongated bubble and the active liquid agitation. As  $5 < 25 \text{ kW/m}^2$  the local coefficient is almost constant. This means that the evaporative mechanism and the liquid agitation is not enough to remove heat from the surface. As  $q''$  increases more than  $25 \text{ kW/m}^2$  upcoming bubbles from the bottom destroy the lower side boundary of the elongated bubble and generates a kind of active mixing movement in the elongated bubble. Thereafter, gradual increase in the local coefficient is obtained. The intensity of the liquid agitation increases much and this regards as the major cause of the increase in heat transfer at higher heat fluxes larger than  $70 \text{ kW/m}^2$ . Through the heat flux regions several photos of pool boiling were taken and some of them are shown in Fig. 6. Comparisons of the present results with Nishikawa et al. (1984) and Jung et al. (1987) as the plate is horizontally facing downward ( $\theta=180^\circ$ ) or upward ( $\theta=0^\circ$ ) show that a similar tendency



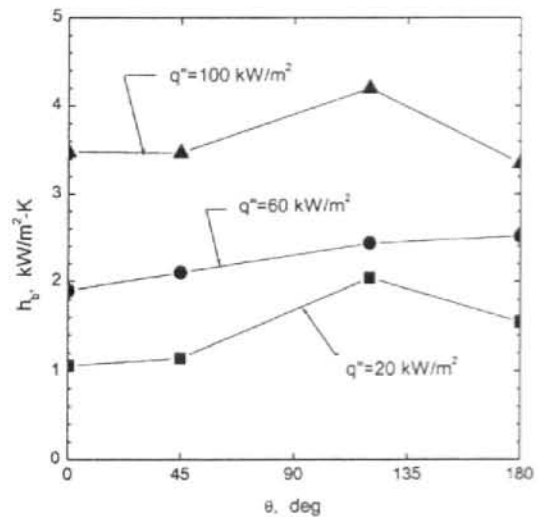
**Fig. 6** Photos of saturated pool boiling on the inside surface

is observed at both tube inside and plate cases. Higher heat transfer coefficients is observed at  $\theta=180^\circ$ . The difference between two coefficients is high at lower heat fluxes and becomes small as the heat flux increases.

Figure 7 shows variations in heat transfer coefficients as the azimuthal angle changes. For the comparison results for three heat fluxes of 20, 60, and 100 kW/m<sup>2</sup> are depicted. The heat transfer coefficients were calculated using curve fitted correlations. The empirical equations for the tube outside and inside have the forms of the first and third order polynomials, respectively, and predict the empirical data within  $\pm 10\%$  error bound. Results for the outside surface show a uniform tendency. However, tendencies for the inside surface are very irregular as the heat flux increases.



(a) Tube outside



(b) Tube inside

**Fig. 7** Curves of  $h_b$  versus  $\theta$  as the heat flux changes

Figure 8 shows graphs of the relative intensity of the related mechanisms due to the azimuthal angle change. In the figure every mechanisms increases heat transfer rate but the bubble coalescence on the surface. The curves shift to the lower azimuthal angles as the heat flux increases.

The local coefficients on the outside and inside surfaces were compared each other at the same azimuthal angle and the results were shown in Fig. 9. Experimental data for the azimuthal angles of 0°, 45°, and 180° have been plotted. The slopes of  $h_b$  versus  $\Delta T_{sat}$  curves for the outside tube

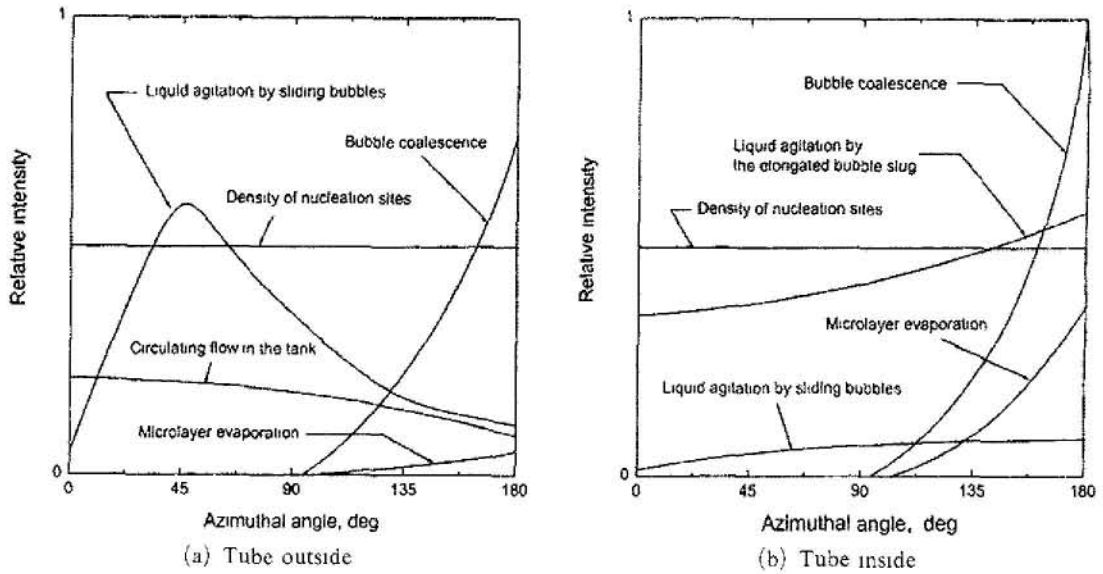


Fig. 8 Schematic of the relative intensity of the mechanisms

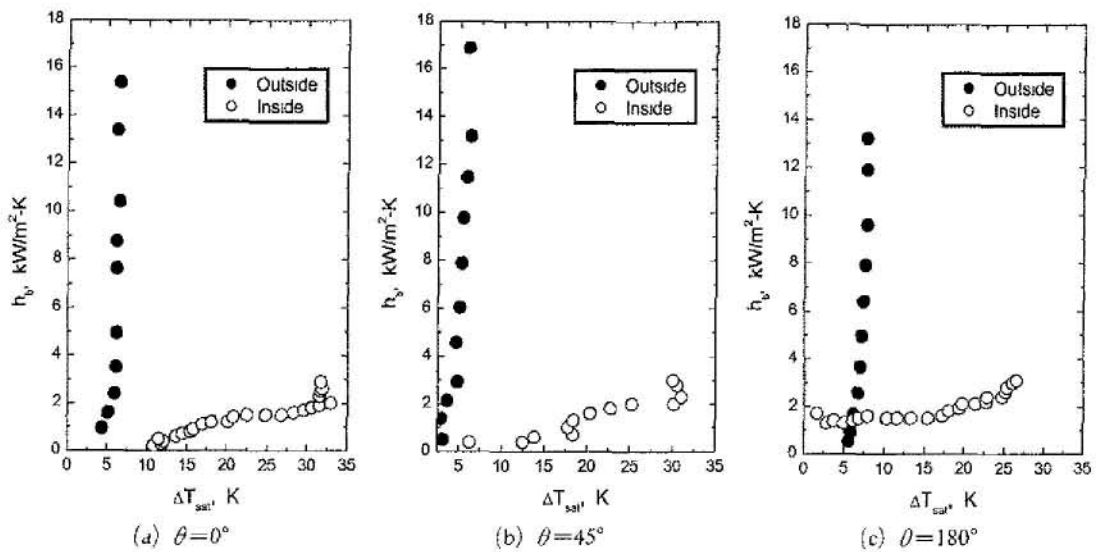


Fig. 9 Comparison of local coefficients for the outside and inside surfaces

are much bigger than the slope for the inside tube. The average slope for the experimental data for the outside surface is 7.4 while the slope is only nearby 0.1 for the inside surface at  $\theta=45^\circ$ . To have the same heat transfer coefficient of  $2 \text{ kW/m}^2\text{-K}$  at  $\theta=0^\circ$  the required wall superheating on the outside surface is only 5.6 K while the value is 33 K on the inside surface. For the inside surface, higher heat transfer coefficient was observed at very lower  $\Delta T_{\text{sat}}$  nearby 0 at

$\theta=180^\circ$ . The departed bubbles from the tube bottom and side regions move upward and coalesce at the uppermost regions of the tube inside to generate a very large elongated bubble underneath the surface. As the bubble flows out of the tube, environmental liquid rushes into the space and, accordingly, active liquid agitation is generated inside the tube. Therefore, the higher heat transfer coefficient at lower heat fluxes can be explained by both of the evaporative mechanism



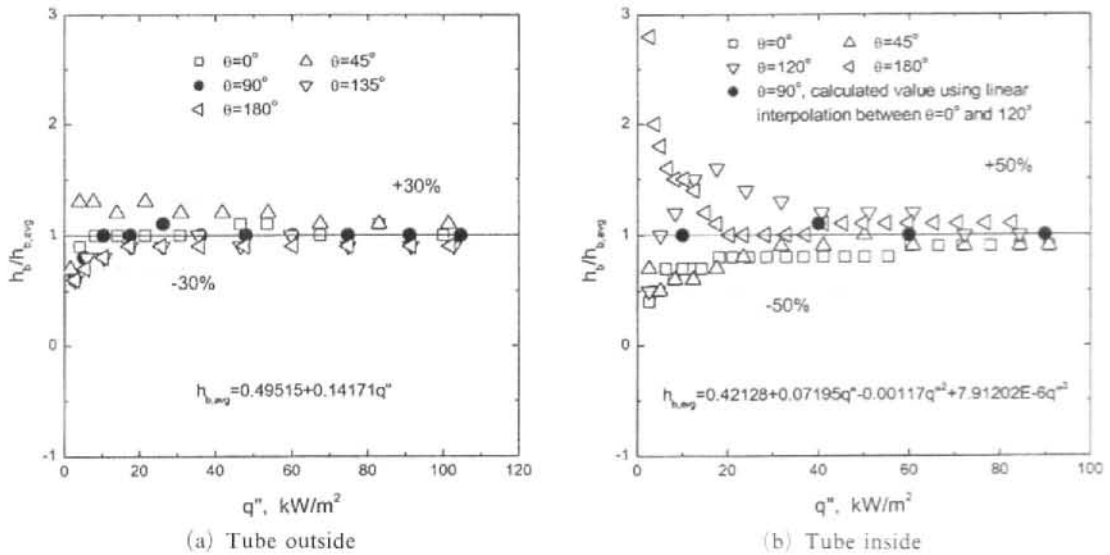


Fig. 10 Comparison of the experimental data with the calculated average values

underneath the elongated bubble and active liquid agitation. As the heat flux increases the intensity of liquid agitation increases much and this regards as the major cause of the increase in heat transfer at higher heat flux.

Experimental data of the outside and inside surfaces have been analyzed to propose a method of predicting average heat transfer coefficients. As shown in the Fig. 10 the measured values at  $\theta=90^\circ$  are nearly same to the calculated values. The equation of the average values has been developed using every experimental data along the tube periphery. Since no experimental data existed at  $\theta=90^\circ$  for the inside surface, the data set were generated through linear interpolation process between  $\theta=45^\circ$  and  $120^\circ$ . Kang's previous results (2000) and Gupta et al.'s results (1995) for the tube located at the bottom position of a bundle showed similar tendency while the diameter of the tubes was 19.05 mm. Therefore, it can be suggested that the local heat transfer coefficient at  $\theta=90^\circ$  can be treated as the average value along the tube circumference of the outside and inside surfaces.

#### 4. Conclusions

Local heat transfer coefficients on the outside

and inside surfaces of a 51 mm diameter horizontal tube have been investigated experimentally in saturated water at atmospheric pressure. The major conclusions of the present study are as follows :

(1) Much variation in local coefficients was observed along the tube periphery. On the outside surface the maximum and the minimum values are observed at  $\theta=45^\circ$  and  $180^\circ$ , respectively. However, on the inside surface only the minimum was observed at the tube bottom.

(2) Major mechanisms on the outside surface are liquid agitation due to sliding bubbles and bubble coalescence while those mechanisms on the inside are micro layer evaporation and liquid agitation by the elongated bubble slug. The micro layer evaporation is most effective at heat fluxes less than  $5 \text{ kW/m}^2$ . As the value of the heat flux increases the mechanism of liquid agitation gets effective both on outside and inside surfaces.

(3) The local heat transfer coefficient measured at  $\theta=90^\circ$  can be recommended as the average value of the tube periphery both on the outside and inside surfaces of the tube.

#### References

Cheung, F. B., Haddad, K. H. and Liu, Y. C.,

- 1999, "Boundary-layer-boiling and Critical-heat-flux Phenomena on a Downward-facing Hemispherical Surface," *Nuclear Technology*, Vol 126, pp 243~264
- Cornwell, K and Einarsson, J G, 1990, "Influence of Fluid Flow on Nucleate Boiling from a Tube," *Experimental Heat Transfer*, Vol 3, pp 101~116
- Cornwell, K and Houston, S D, 1994, "Nucleate Pool Boiling on Horizontal Tubes A Convection-based Correlation," *Int. J. Heat Mass Transfer*, Vol 37 (Suppl 1), pp 303~309
- El-Genk, M S and Gao, C, 1999, "Experiments on Pool Boiling of Water from Downward-facing Hemispheres," *Nuclear Technology*, Vol 125, pp 52~69
- Gupta, A, Sami, J S and Varma, H K, 1995, "Boiling Heat Transfer in Small Horizontal Tube Bundles at Low Cross-flow Velocities," *Int J Heat mass Transfer*, Vol 38(4), pp 599~605
- Hewitt, G F, 1978, "Nucleate Boiling Heat Transfer, Two-phase Flows and Heat Transfer with Application to Nuclear Reactor Design Problems," *Gmoux, J J, ed. Hemisphere Publishing Corporation*, pp 89~109
- Jabardo, J M S and Filho, E P B, 2000, "Convective Boiling of Halocarbon Refrigerants Flowing in a Horizontal Copper Tube—An Experimental Study," *Experimental Thermal and Fluid Science*, Vol 23, pp 93~104
- Jung, D S, Venant, J E S and Sousa, A C M, 1987, "Effects of Enhanced Surfaces and Surface Orientations on Nucleate and Film Boiling Heat Transfer in R-11," *Int J Heat Mass Transfer*, Vol 30(12), pp 2627~2639
- Kang, M G, 2000, "Effect of Tube Inclination on Pool Boiling Heat Transfer," *ASME J Heat Transfer*, Vol 122, pp 188~192
- Kang, M G, 2001, "The Effect of Tube Orientation on Pool Boiling Heat Transfer," *Trans. KSME B*, Vol 24(1), pp 147~151
- Lance, R P and Myers, J E, 1958, "Local Boiling Coefficients on a Horizontal Tube," *AIChE Journal*, Vol 4(1), pp 75~80
- Nishikawa, K, Fujita, Y, Uchida, S and Ohta, H, 1984, "Effect of Surface Configuration on Nucleate Boiling Heat Transfer," *Int. J Heat Mass Transfer*, Vol 27(9), pp 1559~1571